

Berberine and Its More Biologically Available Derivative, Dihydroberberine, Inhibit Mitochondrial Respiratory Complex I

A Mechanism for the Action of Berberine to Activate AMP-Activated Protein Kinase and Improve Insulin Action

Nigel Turner,¹ Jing-Ya Li,^{1,2} Alison Gosby,¹ Sabrina W.C. To,¹ Zhe Cheng,² Hiroyuki Miyoshi,³ Makoto M. Taketo,³ Gregory J. Cooney,¹ Edward W. Kraegen,¹ David E. James,¹ Li-Hong Hu,² Jia Li,² and Ji-Ming Ye¹

OBJECTIVE—Berberine (BBR) activates AMP-activated protein kinase (AMPK) and improves insulin sensitivity in rodent models of insulin resistance. We investigated the mechanism of activation of AMPK by BBR and explored whether derivatization of BBR could improve its in vivo efficacy.

RESEARCH DESIGN AND METHODS—AMPK phosphorylation was examined in L6 myotubes and *LKB1*^{-/-} cells, with or without the Ca²⁺/calmodulin-dependent protein kinase kinase (CAMKK) inhibitor STO-609. Oxygen consumption was measured in L6 myotubes and isolated muscle mitochondria. The effect of a BBR derivative, dihydroberberine (dhBBR), on adiposity and glucose metabolism was examined in rodents fed a high-fat diet.

RESULTS—We have made the following novel observations: 1) BBR dose-dependently inhibited respiration in L6 myotubes and muscle mitochondria, through a specific effect on respiratory complex I, similar to that observed with metformin and rosiglitazone; 2) activation of AMPK by BBR did not rely on the activity of either LKB1 or CAMKK β , consistent with major regulation at the level of the AMPK phosphatase; and 3) a novel BBR derivative, dhBBR, was identified that displayed improved in vivo efficacy in terms of counteracting increased adiposity, tissue triglyceride accumulation, and insulin resistance in high-fat-fed rodents. This effect is likely due to enhanced oral bioavailability.

CONCLUSIONS—Complex I of the respiratory chain represents a major target for compounds that improve whole-body insulin

sensitivity through increased AMPK activity. The identification of a novel derivative of BBR with improved in vivo efficacy highlights the potential importance of BBR as a novel therapy for the treatment of type 2 diabetes. *Diabetes* 57:1414–1418, 2008

Insulin resistance is a major metabolic abnormality leading to type 2 diabetes, and, as such, there is considerable interest in the discovery of insulin-sensitizing agents to aid in the treatment of this disease. AMP-activated protein kinase (AMPK), a heterotrimeric protein that plays a key role in regulation of whole-body energy homeostasis, is one attractive drug target. Two classes of commonly used insulin-sensitizing drugs, thiazolidinediones and biguanides, exert their beneficial effects, at least in part, by activating AMPK (1,2).

Natural products have been a rich resource for the development of novel therapeutics used to treat a variety of human diseases. We have recently reported that berberine (BBR) displays insulin-sensitizing properties in rodent models of insulin resistance and diabetes (3). BBR is commonly used as a nonprescription oral drug in China to treat gut infections and diarrhea with few side effects, and its therapeutic potential for the treatment of diabetes (4) and dyslipidemia (5) in humans has been reported. These beneficial effects are related in part to the ability of BBR to activate AMPK (3,6,7). Here we show that, similar to metformin and rosiglitazone, BBR activates AMPK via inhibition of respiratory complex I of the mitochondrion.

Despite its potent stimulation of AMPK in cell-based assays, an important issue arising from our previous work (3) is that considerably large oral doses (380–560 mg · kg⁻¹ · day⁻¹) of BBR were required for beneficial metabolic effects in rodents. Aiming to improve its therapeutic efficacy, we designed a number of BBR derivatives and show that one such derivative, dihydroberberine (dhBBR), has markedly improved in vivo efficacy in the treatment of insulin-resistant rodents.

RESEARCH DESIGN AND METHODS

Preparation of dihydroberberine. Details of the procedures used to prepare dhBBR are included in a supplemental file available in an online appendix at <http://dx.doi.org/10.2337/db07-1552>.

Cell experiments. Cell culture conditions for *LKB1*^{-/-} mouse embryonic fibroblasts (MEFs) and L6 myotubes were as described previously (3,8). [³H]-2-deoxyglucose uptake was measured in L6 cells according to Cheng et al. (7). For immunoblotting experiments, cell lysates were resolved by SDS-

From the ¹Diabetes and Obesity Research Program, Garvan Institute of Medical Research, Darlinghurst, Australia; the ²Shanghai Institute of Materia Medica, Chinese Academy of Sciences, Shanghai, China; and the ³Department of Pharmacology, Graduate School of Medicine, Kyoto University, Kyoto, Japan.

Corresponding authors: Ji-Ming Ye, PhD, Diabetes and Obesity Research Program, Garvan Institute of Medical Research, 384 Victoria St., Darlinghurst, Sydney, New South Wales 2010, Australia. E-mail: j.ye@garvan.org.au; Jia Li, PhD, or Li-Hong Hu, PhD, Shanghai Institute of Materia Medica, 199 Guo Shou Jing Rd., Zhangjiang Hi-Tech Park, Shanghai 201203, China. E-mail: jli@mail.shnc.ac.cn or simmhull@mail.shnc.ac.cn.

Received for publication 31 October 2007 and accepted in revised form 12 February 2008.

Published ahead of print at <http://diabetes.diabetesjournals.org> on 19 February 2008. DOI: 10.2337/db07-1552.

Additional information for this article can be found in an online appendix at <http://dx.doi.org/10.2337/db07-1552>.

N.T., J-Y.L., and A.G. contributed equally to this work.

ACC, acetyl-CoA carboxylase; AICAR, 5-aminoimidazole-4-carboxamide-1- β -D-ribofuranoside; AMPK, AMP-activated protein kinase; BBR, berberine; CAMKK, Ca²⁺/calmodulin-dependent protein kinase kinase; dhBBR, dihydroberberine; HFD, high-fat diet; MEF, mouse embryonic fibroblast.

© 2008 by the American Diabetes Association.

The costs of publication of this article were defrayed in part by the payment of page charges. This article must therefore be hereby marked "advertisement" in accordance with 18 U.S.C. Section 1734 solely to indicate this fact.

PAGE, transferred to polyvinylidene difluoride membranes, and immunoblotted with antibodies specific for LKB1 (Santa Cruz Biotechnology, Santa Cruz, CA), AMPK, pThr172-AMPK, acetyl-CoA carboxylase (ACC), and pSer79-ACC (Cell Signaling Technology, Beverly, MA).

Animals. Male C57Bl/6J mice (6–8 weeks old) and male Wistar rats (250 g) purchased from the Animal Resources Centre (Perth, Australia) were kept in a temperature-controlled room ($22 \pm 1^\circ\text{C}$) on a 12-h light/dark cycle with free access to water. Animals were randomly assigned to receive either standard control rodent diet or a high-fat diet (HFD) to generate insulin resistance (9,10). Mice and rats were fed for 10 weeks and 4 weeks, respectively, and based on pilot testing for dhBBR in mice, BBR and dhBBR were provided in the HFD at a dose of $100 \text{ mg} \cdot \text{kg}^{-1} \cdot \text{day}^{-1}$ for the final 2 weeks of feeding. All experiments were carried out with the approval of the Garvan Institute Animal Experimentation Ethics Committee, following guidelines issued by the National Health and Medical Research Council of Australia.

Muscle mitochondrial isolation and respiration measurements. Methods describing the mitochondrial isolation and respiration measurements are provided in the supplemental file.

In vivo glucose metabolism. Glucose tolerance tests (2 g/kg glucose i.p.) in mice and euglycemic-hyperinsulinemic clamps in rats (insulin infusion $0.25 \text{ units} \cdot \text{kg}^{-1} \cdot \text{h}^{-1}$) were conducted as previously described (9,10). Tissue triglyceride content was determined using a colorimetric assay kit (Roche Diagnostics, Indianapolis, IN).

Pharmacokinetic analysis. Rats were fasted (12 h) and gavaged with 20 mg/kg BBR or dhBBR, and blood samples were obtained over the subsequent 24 h. Plasma concentrations of BBR and dhBBR were determined by liquid chromatography–tandem mass spectrometry (LC-MS/MS) (11).

Statistical analysis. Results are presented as means \pm SE. One-way ANOVA with Fisher's protected least-square difference post hoc test was used to assess statistical significance between groups. For respiration experiments, the effect of drug treatments are given as a percentage of intra-individual basal values (100%), with *P* values calculated by paired two-tailed *t* tests. *P* \leq 0.05 was regarded as statistically significant.

RESULTS

Role of LKB1 and Ca^{2+} /calmodulin-dependent protein kinase kinase (CAMKK) in the action of BBR.

LKB1 and CAMKK β are two important upstream kinases for AMPK. To determine if activation of AMPK by BBR involves either of these kinases, we first examined the effects of the relatively specific CAMKK inhibitor STO-609 (12) on BBR activation of AMPK in L6 myotubes. The Ca^{2+} ionophore ionomycin increased phosphorylation of AMPK and its downstream target ACC, and this effect was blocked by STO-609 (Fig. 1A). However, the increase in phosphorylation of AMPK and ACC by BBR was unaffected by STO-609, suggesting that CAMKK is not the major AMPK kinase regulated by BBR in L6 cells (Fig. 1A). To examine the role of LKB1 in the activation of AMPK by BBR, we used *LKB1*^{-/-} MEFs (Fig. 1B). BBR caused a robust increase in AMPK and ACC phosphorylation in cells lacking LKB1, as did the AMPK activator AICAR (Fig. 1C). Interestingly, treatment of *LKB1*^{-/-} MEFs with STO-609 blocked the activation of AMPK by ionomycin, 5-aminoimidazole-4-carboxamide-1- β -D-ribofuranoside (AICAR), and BBR (Fig. 1C).

BBR inhibits mitochondrial respiration. We recently reported that BBR increases the AMP-to-ATP ratio in L6 myotubes (7). To investigate whether these changes in nucleotide levels may result from inhibition of cellular respiration, oxygen consumption was examined in L6 myotubes. BBR dose-dependently inhibited respiration in L6 myotubes, with an $\sim 50\%$ inhibition at $15 \mu\text{mol/l}$ (Supplementary Fig. 1). Metformin and rosiglitazone also dose-dependently inhibited respiration in L6 myotubes, with rosiglitazone displaying similar potency to BBR, while metformin was substantially less potent (Supplementary Fig. 1). We next examined whether the inhibitory effect of BBR was manifest at the level of the mitochondria. BBR produced a dose-dependent inhibition of oxygen consumption in isolated muscle mitochondria with complex I–I-

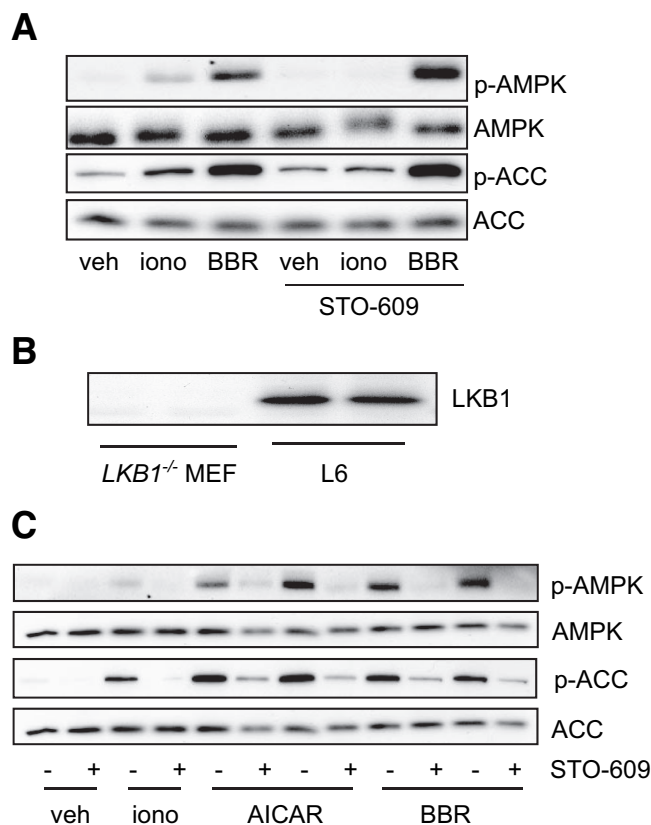


FIG. 1. Effect of CAMKK inhibition and LKB1 deficiency on the activation of AMPK by BBR. **A:** L6 myotubes were incubated for 30 min with vehicle (veh) $1 \mu\text{mol/l}$ ionomycin (iono) or $10 \mu\text{mol/l}$ BBR, with or without preincubation for 1 h with STO-609 ($10 \mu\text{g/ml}$). **B:** LKB1 expression in L6 myotubes and *LKB1*^{-/-} MEFs. **C:** *LKB1*^{-/-} MEFs were incubated for 30 min with $1 \mu\text{mol/l}$ ionomycin, 2 mmol/l AICAR, or $10 \mu\text{mol/l}$ BBR, with or without preincubation for 1 h with STO-609 ($10 \mu\text{g/ml}$). Cells were lysed in $4 \times$ SDS sample buffer, and equal amounts of lysates were resolved by SDS-PAGE and immunoblotted with antibodies specific for LKB1, phospho-AMPK- α (Thr172), total AMPK- α , phospho-ACC (Ser79), and total ACC.

inked substrate (pyruvate), but did not have a substantial effect on complex II–linked respiration using succinate as the substrate (Fig. 2A). A similar inhibitory pattern was also observed in mitochondria for metformin and rosiglitazone (Fig. 2).

dhBBR displays improved in vivo efficacy compared with BBR. Aiming to improve the in vivo efficacy of BBR, we prepared a panel of BBR derivatives and initially tested the effects of these derivatives on glucose uptake and AMPK activation in L6 cells (7). Five of six derivatives had no effect on glucose uptake (Supplementary Fig. 2) or AMPK activation (data not shown). Strikingly, one derivative (dhBBR) displayed similar potency to BBR to stimulate both glucose uptake and AMPK (Supplementary Fig. 2), as well as inhibit respiration in myotubes (Supplementary Fig. 1) and mitochondria (Fig. 2B). A structure-based analysis (using Chemdraw ultra 10 software, <http://www.cambridgesoft.com/services>) suggested that dhBBR would likely display improved in vivo efficacy compared with BBR because of its higher logP value (logP: 3.88 for dhBBR and -0.92 for BBR) (13), and hence its effects were examined in rodent models of insulin resistance.

In mice fed an HFD, treatment with dhBBR ($100 \text{ mg} \cdot \text{kg}^{-1} \cdot \text{day}^{-1}$) markedly reduced adiposity and improved glucose tolerance, compared with HFD controls (Fig. 3). At the same

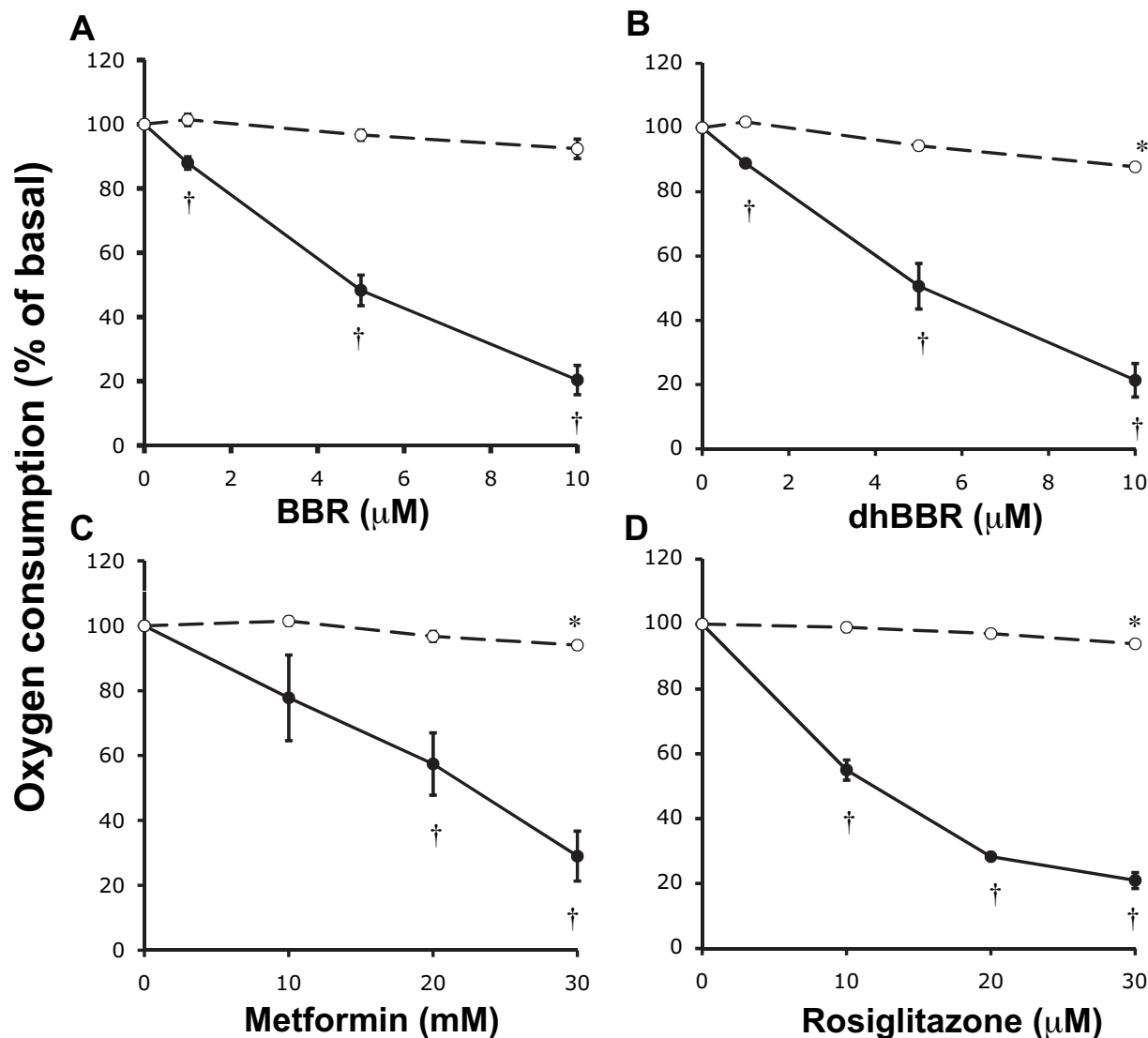


FIG. 2. Inhibition of oxygen consumption in isolated rat muscle mitochondria by BBR (A), dhBBR (B), metformin (C), and rosiglitazone (D). Oxygen consumption rates were measured in mitochondria at 37°C using substrate combinations targeting respiratory complex I (5 mmol/l pyruvate plus 2 mmol/l malate, ●) or complex II (10 mmol/l succinate plus 4 μmol/l rotenone, ○). Data represent means ± SE ($n = 3-6$ per group) and are expressed as a percentage of the basal value (100%). * $P < 0.05$, † $P < 0.01$ vs. basal levels.

dose, BBR had no effect on adiposity or glucose tolerance (Fig. 3), whereas at a dose of 560 mg · kg⁻¹ · day⁻¹ (data not shown), we observed the expected effects of BBR (3).

In HFD rats, treatment with dhBBR resulted in reduced fat pad mass and tissue triglyceride levels compared with HFD controls (Table 1). Whole-body insulin sensitivity, measured as the glucose infusion rate during a hyperinsulinemic-euglycemic clamp, was 44% ($P < 0.01$) higher in dhBBR-treated HFD rats compared with HFD controls, although it was not fully restored to control levels (Table 1). Using glucose tracers, we observed that improvements in whole-body insulin sensitivity in dhBBR-treated HFD rats were largely due to improved uptake of glucose into peripheral tissues, as evidenced by increased R_d and tissue-specific uptake of [³H]-2-deoxyglucose in several tissues (Table 1).

Pharmacokinetic analyses were conducted in rats to determine if enhanced oral bioavailability underpinned the improved in vivo efficacy of dhBBR over BBR. After oral administration of 20 mg/kg BBR, we were unable to detect BBR in the plasma. In contrast, dhBBR at the same oral

dose was rapidly detected in the plasma (Supplementary Fig. 2), displaying a half-life ($t_{1/2}$) of 3.5 ± 1.3 h and a maximum concentration (C_{max}) of 2.8 ± 0.5 ng/ml. Interestingly, in rats gavaged with dhBBR, BBR was also present in the plasma, displaying a longer $t_{1/2}$ (9.6 ± 2.1 h, $P < 0.05$) and a greater C_{max} (12.6 ± 2.4 ng/ml, $P < 0.01$).

DISCUSSION

Here we show that BBR has a similar effect to metformin and rosiglitazone to inhibit respiratory complex I, consistent with previous studies (14–18). These data highlight the importance of complex I as a diabetes target. Inhibition of complex I is likely the main mechanism by which BBR activates AMPK, since we did not observe selective activation of either CAMKKβ or LKB1 by BBR. These findings are consistent with a recent model proposing a major role for AMPK regulation at the level of the AMPK phosphatase in response to metabolic stress (19,20). Finally, we have also identified a novel BBR derivative that

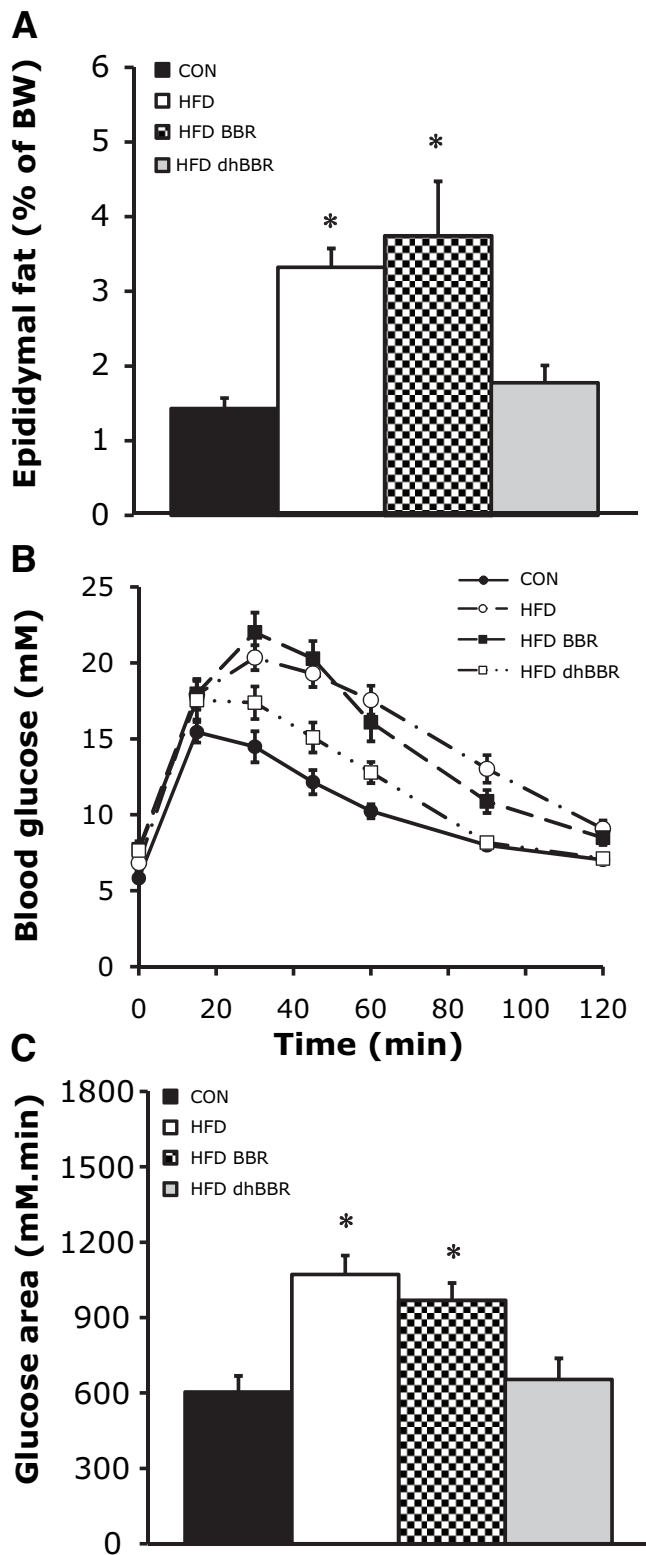


FIG. 3. Effect of BBR and dhBBR on epididymal fat mass and glucose tolerance in mice fed an HFD. BBR or dhBBR were provided in the HFD for 2 weeks at a dose of $100 \text{ mg} \cdot \text{kg}^{-1} \cdot \text{day}^{-1}$. A: Epididymal fat mass expressed as a percentage of body mass. BW, body weight. B: Glucose levels during an intraperitoneal glucose tolerance test (2 g/kg). C: Incremental area under the glucose curve. Data represent the means \pm SE ($n = 5\text{--}15$ mice per group). * $P < 0.01$ vs. control (CON) and dhBBR.

displays improved in vivo efficacy, thus paving a path for future drug development in this area.

The use of $LKB1^{-/-}$ MEFs and the CAMKK inhibitor STO-609 has provided novel insights into the actions of BBR. We observed robust activation of AMPK in $LKB1^{-/-}$ MEFs by BBR, an effect that could be blocked by pretreatment with STO-609. Conversely in L6 myotubes, which express both LKB1 and CAMKK β , we found that STO-609 was unable to block the activation of AMPK by BBR. These findings suggest that in response to BBR, AMPK can be activated via either LKB1 or CAMKK β . We also observed activation of AMPK in $LKB1^{-/-}$ MEFs by the adenosine analog, AICAR, with this effect also abrogated by STO-609. Recently, it was proposed that in addition to a direct allosteric effect, elevated AMP concentrations activate AMPK indirectly by preventing dephosphorylation of Thr172 by phosphatases (19,20). Hence, this model predicts a permissive and/or redundant role for upstream AMPK kinases in metabolic stress-induced AMPK activation, consistent with the present findings for BBR. Interestingly, metformin and rosiglitazone appear to act in an analogous manner (Fig. 2; 16–18). The therapeutic advantage of diverse compounds targeting respiratory complex I is not yet fully appreciated; however, it is noteworthy, in this context, that BBR and metformin have been observed to be beneficial for a broad spectrum of human diseases, including diarrhea, cancer, inflammation, and diabetes (2–4,21–24). We suspect that disturbances in cellular energy homeostasis may be an early event contributing to the therapeutic actions of these compounds.

A potential disadvantage of BBR as an in vivo compound for treatment of diabetes is that we (3) and others (14) have previously reported the need for relatively high doses in rodents to achieve beneficial metabolic effects. In this regard, our identification of a novel derivative that works with substantially improved potency to BBR is a major step forward. At $100 \text{ mg} \cdot \text{kg}^{-1} \cdot \text{day}^{-1}$, dhBBR reduced adiposity and improved glucose tolerance in HFD mice, whereas we observed no effects of BBR at this dose. Furthermore, in HFD rats, the beneficial effects of dhBBR at $100 \text{ mg} \cdot \text{kg}^{-1} \cdot \text{day}^{-1}$ were of a similar magnitude to those previously reported for $380 \text{ mg} \cdot \text{kg}^{-1} \cdot \text{day}^{-1}$ of BBR (3). Examination of the structure of BBR reveals that it possesses an extremely flat configuration, which is likely to have limited absorption across the intestinal epithelia. However, derivatization to dhBBR was predicted to open up the structure, making it more amenable to uptake. Our pharmacokinetics data were consistent with this prediction, with dhBBR displaying improved absorption compared with BBR. Intriguingly, our data also revealed that once absorbed, dhBBR was rapidly converted back to BBR, highlighting the fact that this is likely the active moiety. These findings indicate that dhBBR is in essence an effective vehicle for delivering BBR to the circulation, substantially reducing the oral dose required for beneficial metabolic effects. As BBR has been shown to improve clinical symptoms in patients with type 2 diabetes (4) and dyslipidemia (5), and undesirable side effects have been reported for several popular anti-diabetic drugs (25), dhBBR represents an attractive potential therapy for the treatment of type 2 diabetes and other components of the metabolic syndrome.

ACKNOWLEDGMENTS

This work was supported in part by funding from the Diabetes Australia Research Trust (to E.W.K. and J.-M.Y.),

TABLE 1

Fat pad mass, tissue triglyceride levels, and metabolic parameters from hyperinsulinemic-euglycemic clamps in rats

	Control	HFD	HFD dhBBR
Body mass (g)	349 ± 7	367 ± 5*	361 ± 6
Epididymal fat pad (%)	1.05 ± 0.04	1.94 ± 0.11†	1.48 ± 0.10†§
Inguinal fat pad (%)	1.04 ± 0.07	2.28 ± 0.16†	1.79 ± 0.11†§
Muscle triglyceride (μmol/g)	3.0 ± 0.3	5.1 ± 1.0*	3.1 ± 0.2‡
Liver triglyceride (μmol/g)	4.8 ± 0.2	17.1 ± 1.9†	9.4 ± 1.4*
Glucose infusion rate (mg · kg ⁻¹ · min ⁻¹)	40.2 ± 2.2	19.0 ± 0.4†	27.4 ± 1.9†§
R _d (mg · kg ⁻¹ · min ⁻¹)	38.4 ± 1.9	23.2 ± 0.5†	30.3 ± 0.6†§
Hepatic glucose output (mg · kg ⁻¹ · min ⁻¹)	-1.7 ± 0.5	4.2 ± 0.6†	2.8 ± 1.7†
R _{g'} : red gastrocnemius	35.6 ± 3.3	19.8 ± 1.7†	34.9 ± 7.9‡
R _{g'} : white gastrocnemius	15.2 ± 2.7	5.7 ± 0.7†	8.5 ± 1.5*
R _{g'} : epididymal fat	1.8 ± 0.2	1.3 ± 0.1	2.1 ± 0.4‡

Data are means ± SE ($n = 5-12$ per group). dhBBR was provided in the HFD (100 mg · kg⁻¹ · day⁻¹) for the final 2 weeks of high-fat feeding. Fat pad weights are expressed as a percentage of body mass. Plasma levels of glucose and insulin were similar among the three groups during the clamp (data not shown). R_{g'}, insulin-stimulated glucose uptake during the clamp (μmol/100 g · min). * $P < 0.05$, † $P < 0.01$ vs. control; ‡ $P < 0.05$, § $P < 0.01$ vs. HFD.

International Scientific Linkage Fund of Australia (to E.W.K. and J.-M.Y.), Garvan's Bill Ferris Foundation (to D.E.J.), the Rebecca L. Cooper Medical Research Foundation (to N.T.), the Qi Ming Xing Foundation of Shanghai Ministry of Science and Technology (grant 05QMX1412 to J.-Y.L.), the National Science Foundation Grants of P.R. China (30472045, 30572241, 30623008), and a China-Australia Special Fund (to J.L. and L.-H.H.). N.T. was supported by a Peter Doherty Fellowship and G.J.C., E.W.K., and D.E.J. by the Research Fellowships Scheme of the National Health and Medical Research Council of Australia.

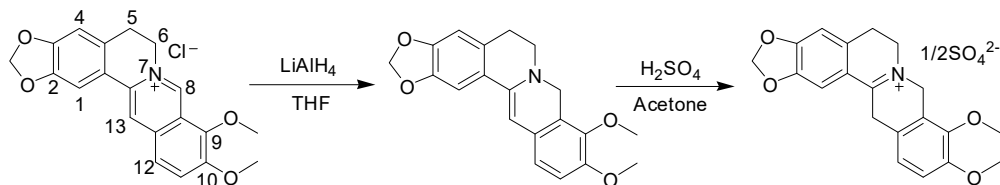
We thank Jennifer Tid-ang and Cordula Hohnen-Behrens for excellent technical assistance and the Biological Testing Facility at the Garvan Institute for help with animal care.

REFERENCES

- Nawrocki AR, Rajala MW, Tomas E, Pajvani UB, Saha AK, Trumbauer ME, Pang Z, Chen AS, Ruderman NB, Chen H, Rossetti L, Scherer PE: Mice lacking adiponectin show decreased hepatic insulin sensitivity and reduced responsiveness to peroxisome proliferator-activated receptor gamma agonists. *J Biol Chem* 281:2654-2660, 2006
- Zhou G, Myers R, Li Y, Chen Y, Shen X, Fenyk-Melody J, Wu M, Ventre J, Doebber T, Fujii N, Musi N, Hirshman MF, Goodyear LJ, Moller DE: Role of AMP-activated protein kinase in mechanism of metformin action. *J Clin Invest* 108:1167-1174, 2001
- Lee YS, Kim WS, Kim KH, Yoon MJ, Cho HJ, Shen Y, Ye JM, Lee CH, Oh WK, Kim CT, Hohnen-Behrens C, Gosby A, Kraegen EW, James DE, Kim JB: Berberine, a natural plant product, activates AMP-activated protein kinase with beneficial metabolic effects in diabetic and insulin-resistant states. *Diabetes* 55:2256-2264, 2006
- Ni YX: Therapeutic effect of berberine on 60 patients with type II diabetes mellitus and experimental research [in Chinese]. *Zhong Xi Yi Jie He Za Zhi* 8:711-713, 1988
- Kong W, Wei J, Abidi P, Lin M, Inaba S, Li C, Wang Y, Wang Z, Si S, Pan H, Wang S, Wu J, Wang Y, Li Z, Liu J, Jiang JD: Berberine is a novel cholesterol-lowering drug working through a unique mechanism distinct from statins. *Nat Med* 10:1344-1351, 2004
- Brusq JM, Ancellin N, Grondin P, Guillard R, Martin S, Saintillan Y, Issandou M: Inhibition of lipid synthesis through activation of AMP kinase: an additional mechanism for the hypolipidemic effects of berberine. *J Lipid Res* 47:1281-1288, 2006
- Cheng Z, Pang T, Gu M, Gao AH, Xie CM, Li JY, Nan FJ, Li J: Berberine-stimulated glucose uptake in L6 myotubes involves both AMPK and p38 MAPK. *Biochim Biophys Acta* 1760:1682-1689, 2006
- Kojima Y, Miyoshi H, Clevers HC, Oshima M, Aoki M, Taketo MM: Suppression of tubulin polymerization by the LKB1-microtubule-associated protein/microtubule affinity-regulating kinase signaling. *J Biol Chem* 282:23532-23540, 2007
- Ye JM, Iglesias MA, Watson DG, Ellis B, Wood L, Jensen PB, Sorensen RV, Larsen PJ, Cooney GJ, Wassermann K, Kraegen EW: PPARalpha/gamma ragaglitazar eliminates fatty liver and enhances insulin action in fat-fed rats in the absence of hepatomegaly. *Am J Physiol Endocrinol Metab* 284: E531-E540, 2003
- Molero JC, Turner N, Thien CB, Langdon WY, James DE, Cooney GJ: Genetic ablation of the c-Cbl ubiquitin ligase domain results in increased energy expenditure and improved insulin action. *Diabetes* 55:3411-3417, 2006
- Chen X, Cui L, Duan X, Ma B, Zhong D: Pharmacokinetics and metabolism of the flavonoid scutellarin in humans after a single oral administration. *Drug Metab Dispos* 34:1345-1352, 2006
- Tokumitsu H, Inuzuka H, Ishikawa Y, Ikeda M, Saji I, Kobayashi R: STO-609, a specific inhibitor of the Ca(2+)/calmodulin-dependent protein kinase kinase. *J Biol Chem* 277:15813-15818, 2002
- Lipinski CA, Lombardo F, Dominy BW, Feeney PJ: Experimental and computational approaches to estimate solubility and permeability in drug discovery and development settings. *Adv Drug Deliv Rev* 46:3-26, 2001
- Yin J, Gao Z, Liu D, Liu Z, Ye J: Berberine improves glucose metabolism through induction of glycolysis. *Am J Physiol Endocrinol Metab* 294: E148-E156, 2008
- Mikes V, Yaguzhinskij LS: Interaction of fluorescent berberine alkyl derivatives with respiratory chain of rat liver mitochondria. *J Bioenerg Biomembr* 17:23-32, 1985
- Owen MR, Doran E, Halestrap AP: Evidence that metformin exerts its anti-diabetic effects through inhibition of complex I of the mitochondrial respiratory chain. *Biochem J* 348:607-614, 2000
- Brunmair B, Staniek K, Gras F, Scharf N, Althaym A, Clara R, Roden M, Gnaiger E, Nohl H, Waldhausl W, Fornsinn C: Thiazolidinediones, like metformin, inhibit respiratory complex I: a common mechanism contributing to their antidiabetic actions? *Diabetes* 53:1052-1059, 2004
- El-Mir MY, Nogueira V, Fontaine E, Averet N, Rigoulet M, Leverve X: Dimethylbiguanide inhibits cell respiration via an indirect effect targeted on the respiratory chain complex I. *J Biol Chem* 275:223-228, 2000
- Suter M, Riek U, Tuerk R, Schlattner U, Wallimann T, Neumann D: Dissecting the role of 5'-AMP for allosteric stimulation, activation, and deactivation of AMP-activated protein kinase. *J Biol Chem* 281:32207-32216, 2006
- Sanders MJ, Grondin PO, Hegarty BD, Snowden MA, Carling D: Investigating the mechanism for AMP activation of the AMP-activated protein kinase cascade. *Biochem J* 403:139-148, 2007
- Kuo CL, Chi CW, Liu TY: The anti-inflammatory potential of berberine in vitro and in vivo. *Cancer Lett* 203:127-137, 2004
- Bulcao C, Ribeiro-Filho FF, Sanudo A, Roberta Ferreira SG: Effects of simvastatin and metformin on inflammation and insulin resistance in individuals with mild metabolic syndrome. *Am J Cardiovasc Drugs* 7:219-224, 2007
- Zakikhani M, Dowling R, Fantus IG, Sonenberg N, Pollak M: Metformin is an AMP kinase-dependent growth inhibitor for breast cancer cells. *Cancer Res* 66:10269-10273, 2006
- Schiller LR: Review article: anti-diarrhoeal pharmacology and therapeutics. *Aliment Pharmacol Ther* 9:87-106, 1995
- Bolen S, Feldman L, Vassy J, Wilson L, Yeh HC, Marinopoulos S, Wiley C, Selvin E, Wilson R, Bass EB, Brancati FL: Systematic review: comparative effectiveness and safety of oral medications for type 2 diabetes mellitus. *Ann Intern Med* 147:386-399, 2007

Supplementary Methods

Preparation of Dihydroberberine.



LiAlH₄ (1.9 g, 50 mmol) was slowly added into a suspension of berberine (3.7 g, 10 mmol) in 100 mL of dry tetrahydrofuran (THF) at 0 °C. The mixture was stirred at room temperature for 3 h and then quenched cautiously by the subsequent addition of H₂O (2 ml), 5 N NaOH (2 ml) and H₂O (6 ml). The mixture was then filtered and the filtrate was evaporated under reduced pressure to remove THF. The residue was re-crystallized with a mixture of methanol and dichloromethane (Shanghai Chemical Plant, Shanghai, P. R. China) to form dihydroberberine (2.4 g, yield 65%). 2.5 ml of 2 N H₂SO₄ was then added into a solution of dihydroberberine (3.4 g, 10 mmol) in 200 ml of acetone over 10 min. The mixture was stirred for 20 min then cooled to 0 °C for 1 h. The mixture was filtered and the filter cake washed with acetone and water respectively. Finally, the filter cake was dried overnight to give dihydroberberine sulfate [5,6-Dihydro-9,10-dimethoxybenzo(g)-1,3-benzodioxolo(5,6-a) quinolinizinium sulfate] (2.9 g, yield 75%).

Muscle Mitochondrial Isolation. For mitochondrial isolation, red quadriceps muscle obtained from control rats was placed in ice-cold mitochondrial isolation medium (in

mM): 100 sucrose, 100 KCl, 50 Tris-HCl, 1 KH₂PO₄, 0.1 EGTA, 0.2% fatty acid free BSA, pH 7.0. Muscle was chopped finely and incubated with shaking at 4°C in isolation medium containing protease (Nagarse, 1.5 mg/g tissue) for 2 min. The nagarse was then diluted 4-fold and samples were immediately homogenized with a Polytron[®] Homogenizer (Kinematica, Lucerne, Switzerland), for 15 sec at the lowest speed. The homogenate was centrifuged at 800 g at 4°C for 5 min to remove nuclei and cell debris. The supernatant was removed and centrifuged at 10,500 g at 4°C for 10 min. The pellet was washed and recentrifuged at 10,500 g at 4°C for 10 min and the resulting pellet, containing mitochondria, was resuspended in respiration medium (see below) at a concentration of 2 ml per milligram of original tissue. Protein content in mitochondria and all cell preparations was measured using the Bradford method.

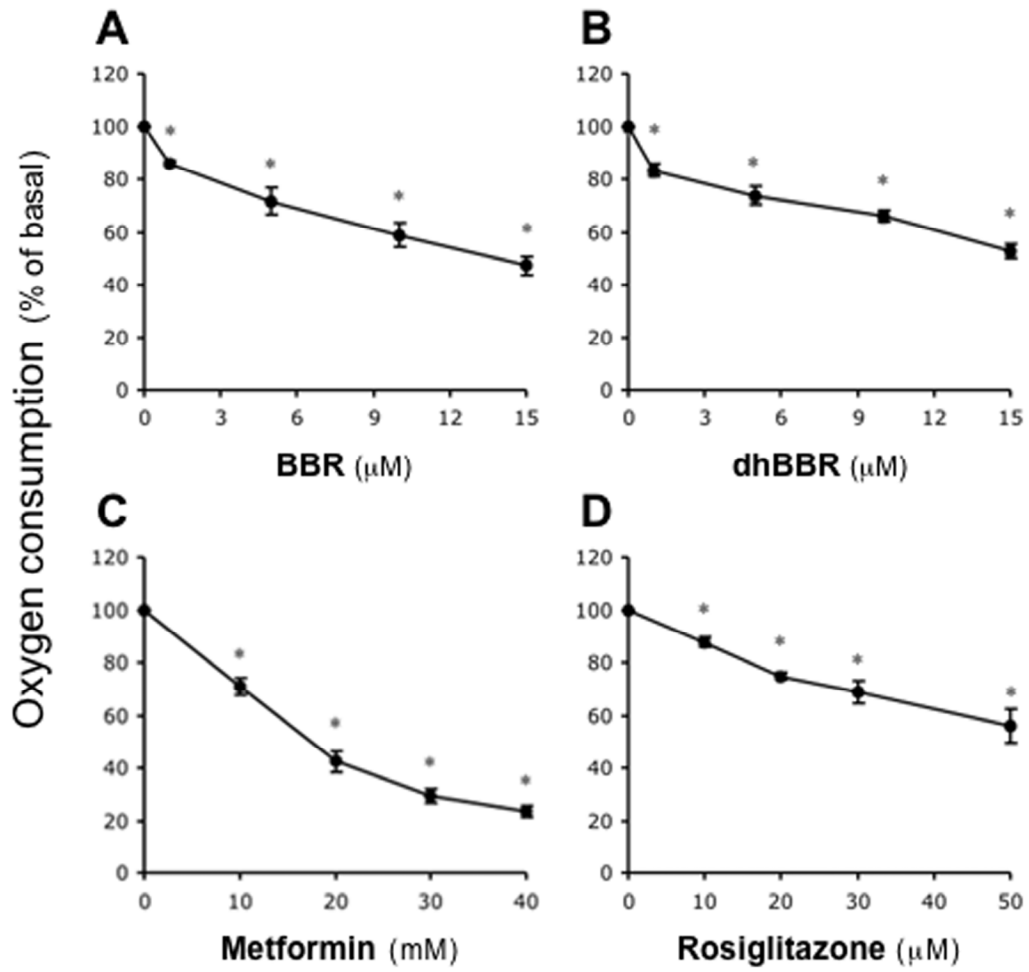
Respiration measurements. Respiration measurements in L6 myotubes and isolated mitochondria were conducted at 37°C in a Clark type oxygen electrode (Strathkelvin Instruments, Motherwell, Scotland). For L6 myotubes (1 – 2 mg protein) the respiration medium consisted of 25 mM glucose, 1 mM pyruvate, 2% BSA in PBS, pH 7.4. Cells were transferred to the electrode chamber and following attainment of a steady rate of oxygen consumption, BBR, dhBBR, metformin (MP Biomedicals, Irvine, CA, USA) or rosiglitazone (a gift from Novo Nordisk, Måløv, Denmark) were added dose-dependently and their effect on oxygen consumption recorded. For mitochondria, the respiration medium contained (in mM): 225 mannitol, 75 sucrose, 10 Tris-HCl, 10 KH₂PO₄, 10 KCl, 0.8 MgCl₂, 0.1 EDTA, 0.3% fatty acid free BSA,

pH 7.0 and the respiratory control ratios (state III/state IV respiration) determined with 5 mM pyruvate as substrate, were approximately 5, indicating well coupled mitochondria. Dose-response effects of the different compounds on mitochondrial respiration were determined in the presence of excess ADP (2.4 mM), using substrate combinations targeting either Complex I (5 mM pyruvate plus 2 mM malate) or Complex II (10 mM succinate plus 4 μ M rotenone) of the respiratory chain.

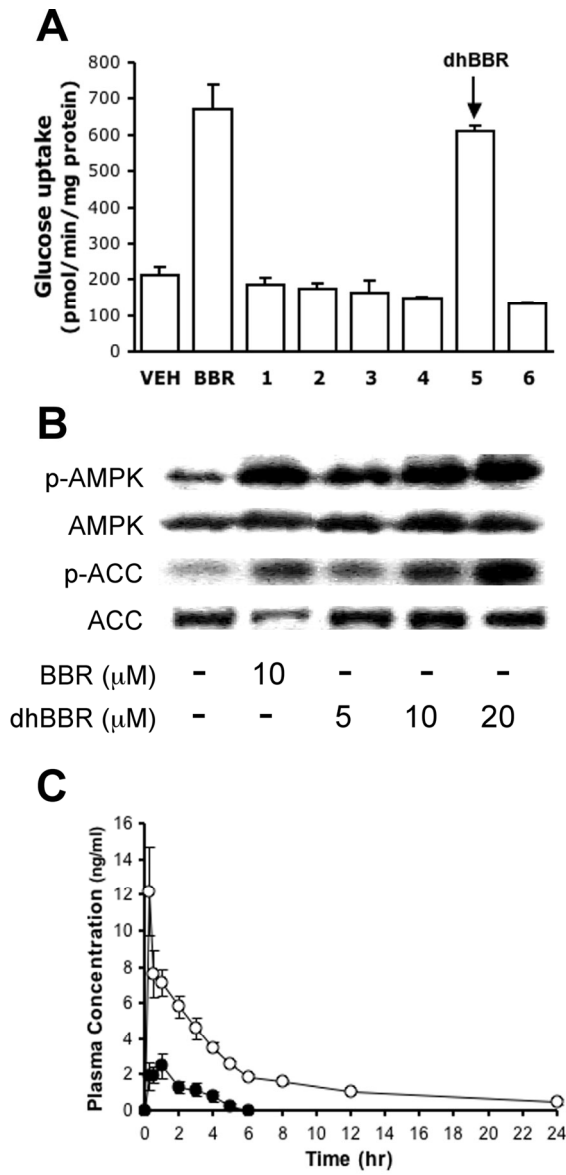
Supplementary Figure Legends

Supplementary Fig 1. Inhibition of oxygen consumption in L6 myotubes by (A) BBR, (B) dhBBR, (C) metformin and (D) rosiglitazone. Oxygen consumption rates were measured in myotubes and are expressed as a percentage of the basal value (=100%). Data represent means \pm SE (n = 6-8 per group). *P < 0.01 vs. basal levels.

Supplementary Fig 2. Stimulation of glucose uptake and AMPK phosphorylation in L6 myotubes by dhBBR and pharmacokinetic analysis of dhBBR in rats. **A)** Glucose uptake measured in L6 myotubes pretreated for 3 hr with 5 μ M BBR and a range of BBR derivatives (compounds 1-6). Data represents mean \pm SE of 2 independent experiments **B)** L6 myotubes were incubated for 30 min with BBR or dhBBR at the indicated concentrations, lysed in 4 x SDS sample buffer and equal amounts of lysates were resolved by SDS PAGE and immunoblotted with antibodies specific for phospho-AMPK- α (Thr172), total AMPK- α , phospho-ACC (Ser79) and total ACC. **C)** Plasma concentration of dhBBR (closed circles) and BBR (open circles) in rats following oral gavage of 20 mg/kg dhBBR. Data represent means \pm SE (n=4).



Supplementary Fig 1



Supplementary Fig 2